

Comparison of dynamical dark energy with Λ CDM in light of DESI DR2

A.N. Ormondroyd,^{1,2*} W.J. Handley,^{1,2} M.P. Hobson¹ and A.N. Lasenby^{1,2}

¹*Astrophysics Group, Cavendish Laboratory, J.J. Thomson Avenue, Cambridge, CB3 0HE, UK*

²*Kavli Institute for Cosmology, Madingley Road, Cambridge, CB3 0HA, UK*

Accepted XXX. Received YYY; in original form ZZZ

ABSTRACT

We present an updated reconstruction of the dark energy equation of state, $w(a)$, using the newly released DESI DR2 Baryon Acoustic Oscillation (BAO) data in combination with Pantheon+ and DES5Y Type Ia supernovae measurements, respectively. Building on our previous analysis in Ormondroyd et al. (2025), which employed a nonparametric flexknot reconstruction approach, we examine whether the evidence for dynamical dark energy persists with the improved precision of the DESI DR2 dataset. We find that while the overall qualitative structure of $w(a)$ remains consistent with our earlier findings, the statistical support for dynamical dark energy is reduced when considering DESI DR2 data alone, particularly for more complex flexknot models with higher numbers of knots. However, the evidence for simpler dynamical models, such as w CDM and CPL (which correspond to $n = 1$ and $n = 2$ knots respectively), increases relative to Λ CDM with DESI DR2 alone, consistent with previous DESI analyses. When combined with Pantheon+ data, the conclusions remain broadly consistent with our earlier work, but the inclusion of DES5Y supernovae data leads to an increase of preference for flexknot models with more than two knots, placing w CDM and CPL on par with Λ CDM.

Key words: methods: statistical – cosmology: dark energy, cosmological parameters

1 INTRODUCTION

The standard model of cosmology, Λ CDM, has been remarkably successful in explaining a wide range of cosmological observations.

Recent work has reinforced the importance of understanding the nature of dark energy through increasingly precise cosmological measurements. In our previous study (Ormondroyd et al. 2025), we employed a nonparametric flexknot reconstruction (originally termed ‘nodal reconstruction’ Vázquez et al. 2012a,b) of the dark energy equation-of-state parameter, $w(a)$, to explore the possibility of dynamical dark energy. Using a flexible linear-spline approach with free-moving nodes, our analysis of DESI Baryon Acoustic Oscillation (BAO) combined with either Pantheon+ or DES5Y Type Ia supernovae data unexpectedly revealed a W-shaped structure in $w(a)$. This structure, which deviates from the conventional constant- w (Λ CDM) picture, raised questions about whether standard parameterisations such as w CDM or CPL might be too restrictive to capture the true dynamical behavior of dark energy. This is acknowledged in the DESI DR2 release (DESI Collaboration et al. 2025d,b,a), which includes an entire paper dedicated to an extended dark energy analysis (DESI Collaboration et al. 2025c).

In this update, we investigate how the conclusions of Ormondroyd et al. (2025) change in light of DESI DR2.

2 DATA

We combine DESI DR2 BAO data with Pantheon+ (Brout et al. 2022) and DES5Y supernovae (DES Collaboration et al. 2024), respectively. DESI DR2 cosmological distances are used as they appear in Table IV of DESI Collaboration et al. (2025a). DESI DR1, Pantheon+, and DES5Y data are used in precisely the same manner as in Ormondroyd et al. (2025).

The DESI DR2 BAO improves constraints on cosmic expansion with a larger dataset of galaxies and quasars than DR1. In addition to the tightening of the error bars compared to the previous release, the Quasar Sample (QSO) now has sufficient signal-to-noise ratio that separate measurements of $D_M(z)$ and $D_H(z)$ are reported in DR2, whereas in DR1 only a volume-averaged $D_V(z)$ value was reported (DESI Collaboration et al. 2025a, 2024a).

3 METHODS

With these improved DESI DR2 measurements now available, we recap the flexknot-based methodology that enables us to explore dynamical dark energy in a nonparametric way. In this approach, $w(a)$ is modelled using a flexible linear spline between free-moving nodes. This technique is well-established in multiple fields within cosmology: it has been used to reconstruct history of the dark energy equation of state from CMB data (Hee et al. 2016; Vázquez et al. 2012b), the primordial power spectrum (Handley et al. 2019; Vázquez et al.

* E-mail: ano23@cam.ac.uk

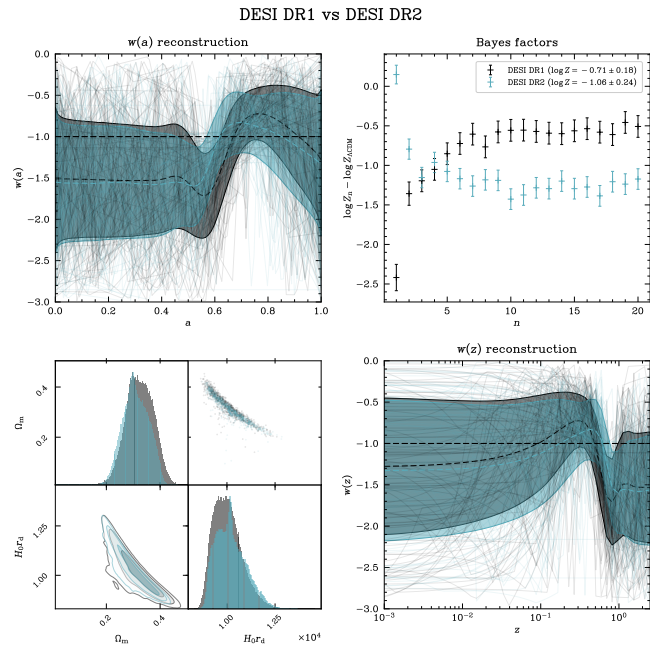


Figure 1. Flexknot reconstruction of $w(a)$ using DESI DR2 BAO data using flexknots, compared to DR1. Upper left panel: the reconstructed $w(a)$. The dashed line is the mean of the posterior, and the shaded region is the 1σ contour. The overall shape is similar to DR1, but the transition around $a = 0.6 - 0.7$ is less pronounced. Upper right panel: the evidence for each number of knots n , relative to Λ CDM. The biggest change is the new data admits a constant w model ($n = 1$) as a viable model. Evidence for models with more than four knots is reduced compared to DR1. Lower left panel: posterior distributions of Ω_m and $H_0 r_d$. Lower right panel: the same reconstruction as the upper left panel, but transformed to $w(z)$.

2012a; Aslanyan et al. 2014; Finelli et al. 2018; Planck Collaboration et al. 2014, 2016), the cosmic reionisation history (Millea & Bouchet 2018; Heimersheim et al. 2022), galaxy cluster profiles (Olamaie et al. 2018), and the 21 cm signal (Heimersheim et al. 2024; Shen et al. 2024). Unlike dark energy reconstructions such as Gaussian processes Dinda & Maartens (2025); Yang et al. (2025); Johnson & Jassal (2025); Gao et al. (2025) or cubic splines (Berti et al. 2025), flexknots can reconstruct arbitrarily sharp features, and have extremely weak functional correlation structure. Flexknots also have the advantage that the w CDM and CPL models correspond to the special cases of $n = 1$ and $n = 2$ knots, respectively.

Posterior samples and evidences were obtained using the nested sampling algorithm PolyChord (Skilling 2004; Handley et al. 2015a,b). A branch of fgivenx was used to produce the functional posterior plots (Handley 2019a), and anesthetic was used to process the nested sampling chains (Handley 2019b).

As in Ormondroyd et al. (2025), H_0 and M_B are marginalised over, and the prior on M_B is taken to be uniform and sufficiently wide to contain the entire posterior. In the DESI analyses DESI Collaboration et al. (2025a, 2024b), it is enforced that $w_0 + w_a < 0$ to ensure that there is a period of matter domination at high redshifts. In this work, we take $w_i < 0$ to achieve the same effect.

Table 1 lists the cosmological priors used in this work, the same as Ormondroyd et al. (2025), which themselves were chosen to remain consistent with those used in Calderon et al. (2024).

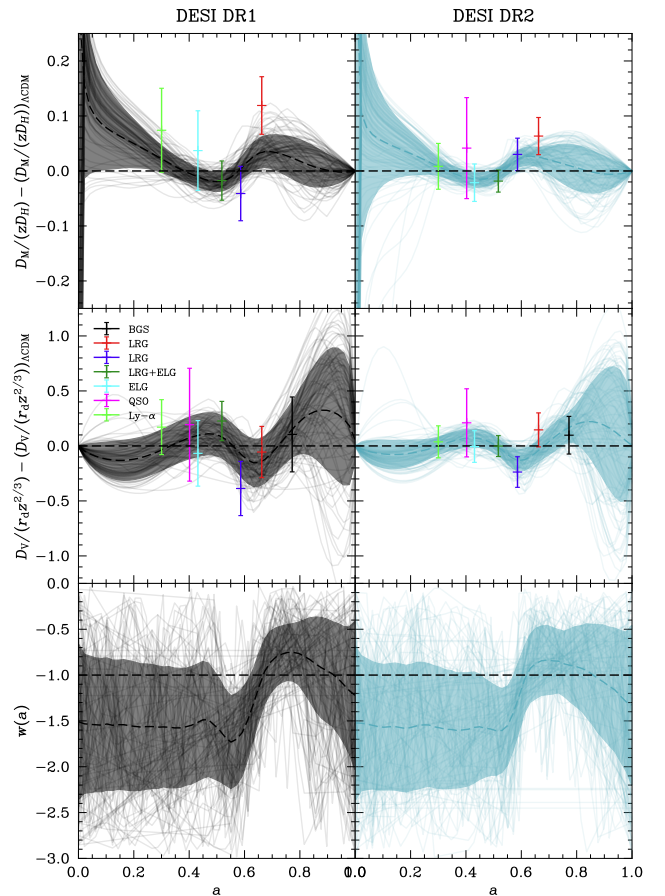


Figure 2. BAO distances reconstructed from DESI BAO data. The left column is DESI DR1, the right column is DESI DR2. The best-fit Λ CDM has been subtracted from each set of distances, and the $w(a)$ posteriors are repeated in the bottom two panels. 1σ contours are also shown. It can be seen how the smaller error bars in DR2 have produced a narrower 1σ contour for the reconstructions.

4 RESULTS

Figure 1 shows reconstructions of $w(a)$ from DESI alone, and compares DR1 and DR2. Figure 2 shows the corresponding BAO distances reconstructed from DESI BAO data, compared to the best-fit Λ CDM model. The most significant change is not in the shape of the $w(a)$ posterior, but the evidences for each number of knots in the reconstruction. The greatest contrast is in the single knot case (w CDM), for which there is now a very slight preference relative to Λ CDM in DR2, whereas w CDM was reasonably disfavoured in DR1. As the number of knots increases, the evidences tend to a lower value for DR2 than for DR1. This means that DR2 is less supportive than DR1 of the flexknot model.

The most significant change to the reconstructed $w(a)$ is the transition around $a = 0.6 - 0.7$, which is the region containing the two LRG points whose affect was investigated in detail in Ormondroyd et al. (2025). This has moved to slightly higher redshifts, and is tighter than in DR1. The DR2 reconstructions have a more pronounced transition at slightly higher redshifts between phantom and quintessence than DR1, which continues to be the case when supernovae are included.

Looking specifically, however, at $n = 2$ (i.e. the CPL parameterisation), we note that the evidence slightly increases relative to Λ CDM with DR2 compared to DR1. This matches the conclusion of DESI

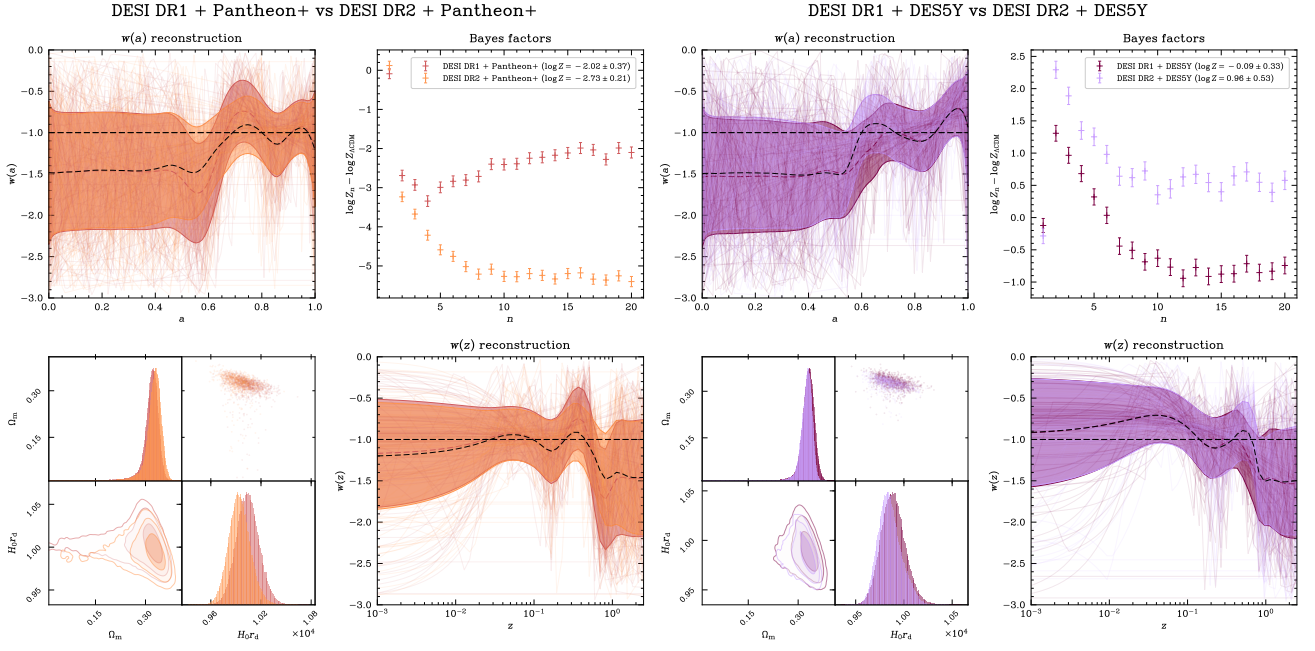


Figure 3. Similar to Figure 1, but comparing DESI DR2 BAO data with Pantheon+ supernovae (left) and DES5Y supernovae (right). The most significant difference between the DR1 and DR2 reconstructions is the same region of a as in Figure 1. Left four panels: DESI DR2 + Pantheon+, compared to DR1 + Pantheon+. The evidence for w CDM is very similar between DR1 and DR2, but the remaining flexknots are less favoured in DR2. Right four panels: DESI DR2 + DES5Y, compared to DR1 + DES5Y. The change is very much the opposite as it was with Pantheon+, with the evidence for all numbers of knots greater than or equal to two have increased significantly, with CPL remaining the preferred model.

| Parameter | Prior |
|-----------------------|----------------------------|
| n | [1, 20] |
| a_{n-1} | 0 |
| a_{n-2}, \dots, a_1 | sorted($[a_{n-1}, a_0]$) |
| a_0 | 1 |
| w_{n-1}, \dots, w_0 | $[-3, -0.01]$ |
| Ω_m | [0.01, 0.99] |
| $H_0 r_d$ (DESI) | [3650, 18250] |
| H_0 (1a) | [20, 100] |

Table 1. Cosmological priors used in this work. Fixed values are indicated by a single number, while uniform priors are denoted by brackets. As BAO only depend on the product $H_0 r_d$, and supernovae depend on H_0 , those parameters are only included as necessary. Whilst the dynamical dark energy priors are broadly consistent with those in DESI Collaboration et al. (2025a), these inevitably differ from CPL priors which instead put a uniform prior on the gradient w_a .

Collaboration et al. (2025a) that DR2 more strongly supports CPL dark energy over Λ CDM than DR1, although the overall evidence for both flexknots, and CPL, is marginal.

Figure 3 shows a comparison of results from the DESI DR1/DR2 BAO data when combined with Pantheon+ and DES5Y supernovae, respectively. The evidences for w CDM in DR2 are very similar to those with DR1 and, as when using DESI alone, the evidences tend to a lower value for DR2 than for DR1 as the number of knots n increases. Most notably, there is now a preference for models with large numbers of knots with DESI DR2 + DES5Y, which was the only combination in Ormondroyd et al. (2025) which had any evidence in favour of dynamical dark energy, and the CPL model is still favoured.

When combining data it is prudent to check that the datasets are consistent with each other. Here we follow Ormondroyd et al. (2025) in using the tension analysis developed and deployed in Handley & Lemos (2019); Hergt et al. (2021); Ormondroyd et al. (2023) via

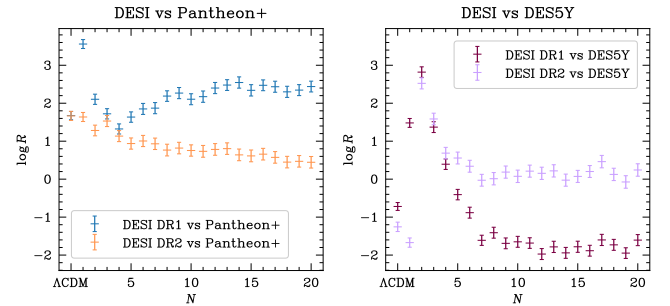


Figure 4. Tension quantifications between combinations of datasets. For each knot reconstruction N we compare the tension between DESI (DR1 or DR2) and supernovae (Pantheon+ [left panel] or DES5Y [right panel]). In light of the update from DR1 to DR2, the tension has increased between DESI and Pantheon+ ($\log R$ lower), but remains consistent ($\log R > 0$). For DESI and DES5Y in light of the update from DR1 to DR2 the tension has decreased ($\log R$ higher) and is now consistent $\log R > 0$ for all but the Λ CDM ($N = 0$) and w CDM ($N = 1$) cases.

the $\log R$ statistic. In Figure 4 we show the tension quantifications between DESI and supernovae datasets. For DESI vs Pantheon+, there has been a slight increase in tension between DR1 and DR2, but they remain consistent. For DESI vs DES5Y the tension has decreased between DR1 and DR2, and is now consistent for all but the Λ CDM and w CDM cases. In this sense, dynamical dark energy models can be viewed as resolving a discrepancy between DESI and DES5Y data, in addition to providing a better fit to the data.

For reference, we show the non-overlaid reconstructions of $w(a)$ for the remaining combinations of datasets in Figure 5. DESI alone can be seen in the lower panels of Figure 2.

5 CONCLUSIONS

We revisited the dynamical dark energy reconstructions presented in Ormondroyd et al. (2025) using the newly-released DESI DR2 BAO data in combination with Pantheon+ and DES5Y supernovae measurements, respectively. Our analysis employed a flexknot methodology to reconstruct the evolution of the dark energy equation of state $w(a)$. Overall, we find that while the qualitative shape of the reconstructed $w(a)$ remains consistent with our previous work, there is a marked change in the statistical evidence for dynamical dark energy.

The DESI DR2 data alone lead to a reduction in the evidence as compared with DR1 for flexknot models with larger numbers of knots. However, the evidence for the w CDM and CPL models, which correspond to $n = 1$ and $n = 2$ knots respectively, have increased compared to Λ CDM with DESI alone, which aligns with the conclusions of DESI Collaboration et al. (2025a). When the DESI DR2 BAO data are combined with Pantheon+ supernovae, the conclusions are similar to those in our original work.

However, with DES5Y supernovae, there is now increased evidence for models with a larger number of knots, with evidence for CPL, which remains the preferred model, also increasing, and with w CDM remaining on-par with Λ CDM. In addition to providing a better fit, dynamical dark energy models serve to resolve a discrepancy between DESI and DES5Y data.

ACKNOWLEDGEMENTS

This work was performed using the Cambridge Service for Data Driven Discovery (CSD3), part of which is operated by the University of Cambridge Research Computing on behalf of the STFC DiRAC HPC Facility (www.dirac.ac.uk). The DiRAC component of CSD3 was funded by BEIS capital funding via STFC capital grants ST/P002307/1 and ST/R002452/1 and STFC operations grant ST/R00689X/1. DiRAC is part of the National e-Infrastructure.

The tension calculations in this work made use of NumPy (Harris et al. 2020), SciPy (Virtanen et al. 2020), and pandas (The pandas development team 2023; McKinney 2010). The plots were produced in matplotlib (Hunter 2007), using the smplotlib template created by Li (2023).

DATA AVAILABILITY

The pared-down Python pipeline and nested sampling chains used in this work can be obtained from Zenodo (Ormondroyd 2025).

REFERENCES

Aslanyan G., Price L. C., Abazajian K. N., Easter R., 2014, *J. Cosmology Astropart. Phys.*, 2014, 052
 Berti M., Bellini E., Bonvin C., Kunz M., Viel M., Zumalacarregui M., 2025, arXiv e-prints, p. arXiv:2503.13198
 Brout D., et al., 2022, *ApJ*, 938, 110
 Calderon R., et al., 2024, *J. Cosmology Astropart. Phys.*, 2024, 048
 DES Collaboration et al., 2024, *ApJ*, 973, L14
 DESI Collaboration et al., 2024a, arXiv e-prints, p. arXiv:2404.03000
 DESI Collaboration et al., 2024b, arXiv e-prints, p. arXiv:2404.03002
 DESI Collaboration et al., 2025a, arXiv e-prints, p. arXiv:2503.14738
 DESI Collaboration et al., 2025b, arXiv e-prints, p. arXiv:2503.14739
 DESI Collaboration et al., 2025c, arXiv e-prints, p. arXiv:2503.14743
 DESI Collaboration et al., 2025d, arXiv e-prints, p. arXiv:2503.14745
 Dinda B. R., Maartens R., 2025, *J. Cosmology Astropart. Phys.*, 2025, 120

Finelli F., et al., 2018, *J. Cosmology Astropart. Phys.*, 2018, 016
 Gao S., Gao Q., Gong Y., Lu X., 2025, arXiv e-prints, p. arXiv:2503.15943
 Handley W., 2019a, fgivex: Functional posterior plotter, Astrophysics Source Code Library, record ascl:1909.014
 Handley W., 2019b, *The Journal of Open Source Software*, 4, 1414
 Handley W., Lemos P., 2019, *Phys. Rev. D*, 100, 043504
 Handley W. J., Hobson M. P., Lasenby A. N., 2015a, *MNRAS*, 450, L61
 Handley W. J., Hobson M. P., Lasenby A. N., 2015b, *MNRAS*, 453, 4384
 Handley W. J., Lasenby A. N., Peiris H. V., Hobson M. P., 2019, *Phys. Rev. D*, 100, 103511
 Harris C. R., et al., 2020, *Nature*, 585, 357
 Hee S., Handley W. J., Hobson M. P., Lasenby A. N., 2016, *MNRAS*, 455, 2461
 Heimersheim S., Sartorio N. S., Fialkov A., Lorimer D. R., 2022, *ApJ*, 933, 57
 Heimersheim S., Rønneberg L., Linton H., Pagani F., Fialkov A., 2024, *MNRAS*, 527, 11404
 Hergt L. T., Handley W. J., Hobson M. P., Lasenby A. N., 2021, *Phys. Rev. D*, 103, 123511
 Hunter J. D., 2007, *Computing in Science & Engineering*, 9, 90
 Johnson J. P., Jassal H. K., 2025, arXiv e-prints, p. arXiv:2503.04273
 Li J., 2023, AstroJacobLi/smplotlib: v0.0.9, doi:10.5281/zenodo.8126529, <https://doi.org/10.5281/zenodo.8126529>
 McKinney W., 2010, in Stéfan van der Walt Jarrod Millman eds, Proceedings of the 9th Python in Science Conference. pp 56 – 61, doi:10.25080/Majora-92bf1922-00a
 Millea M., Bouchet F., 2018, *A&A*, 617, A96
 Olamaie M., Hobson M. P., Feroz F., Grainge K. J. B., Lasenby A., Perrott Y. C., Rumsey C., Saunders R. D. E., 2018, *MNRAS*, 481, 3853
 Ormondroyd A., 2025, Nonparametric reconstructions of dynamical dark energy using flexknots, doi:10.5281/zenodo.15025604, <https://doi.org/10.5281/zenodo.15025604>
 Ormondroyd A. N., Handley W. J., Hobson M. P., Lasenby A. N., 2023, arXiv e-prints, p. arXiv:2310.08490
 Ormondroyd A. N., Handley W. J., Hobson M. P., Lasenby A. N., 2025, arXiv e-prints, p. arXiv:2503.08658
 Planck Collaboration et al., 2014, *A&A*, 571, A22
 Planck Collaboration et al., 2016, *A&A*, 594, A20
 Shen E., Anstey D., de Lera Acedo E., Fialkov A., 2024, *MNRAS*, 529, 1642
 Skilling J., 2004, in Fischer R., Preuss R., Toussaint U. V., eds, American Institute of Physics Conference Series Vol. 735, Bayesian Inference and Maximum Entropy Methods in Science and Engineering: 24th International Workshop on Bayesian Inference and Maximum Entropy Methods in Science and Engineering. pp 395–405, doi:10.1063/1.1835238
 The pandas development team 2023, pandas-dev/pandas: Pandas, doi:10.5281/zenodo.8092754, <https://doi.org/10.5281/zenodo.8092754>
 Vázquez J. A., Bridges M., Hobson M. P., Lasenby A. N., 2012a, *J. Cosmology Astropart. Phys.*, 2012, 006
 Vázquez J. A., Bridges M., Hobson M. P., Lasenby A. N., 2012b, *J. Cosmology Astropart. Phys.*, 2012, 020
 Virtanen P., et al., 2020, *Nature Methods*, 17, 261
 Yang Y., Wang Q., Li C., Yuan P., Ren X., Saridakis E. N., Cai Y.-F., 2025, arXiv e-prints, p. arXiv:2501.18336

This paper has been typeset from a $\text{\TeX}/\text{\LaTeX}$ file prepared by the author.

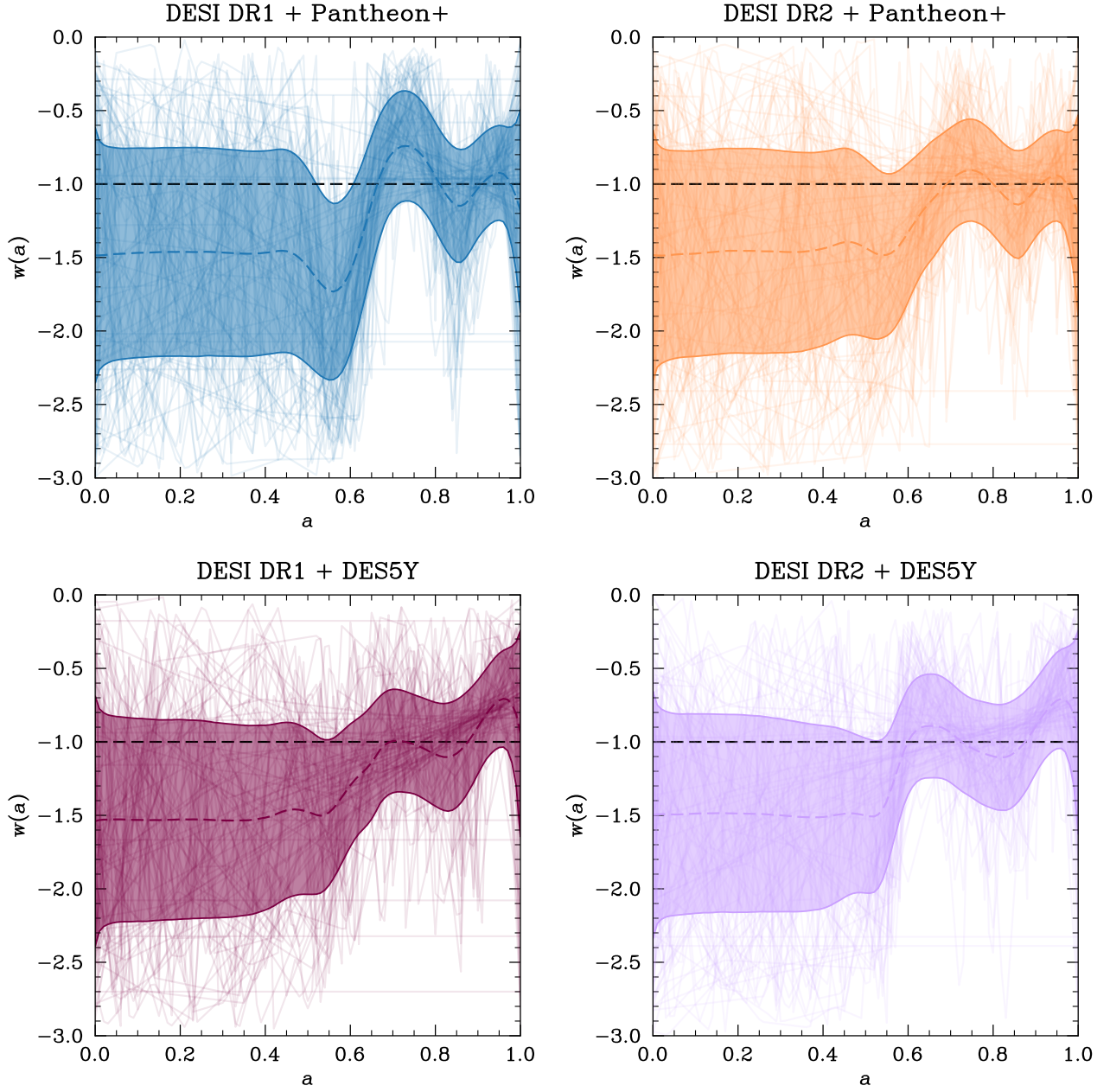


Figure 5. For reference, non-overlaid reconstructions of $w(a)$ for the remaining combinations of datasets, as in the lower panels of Figure 2.